Fundamentals and Applications of Mo and Nb Alloying in High Performance Steels – Volume 1
Edited by Hardy Mohrbacher
CBMM, IMOA and TMS, 2014

THE EFFECT OF NIOBIUM ADDITIONS ON THE MICROSTRUCTURAL MORPHOLOGY IN THE HEAT-AFFECTED ZONE OF LOW-CARBON STEELS

J.R. Yang[1] and C.Y. Huang[2]

[1]Department of Materials Science and Engineering, National Taiwan University,
1 Roosevelt Rd., Sec. 4, Taipei, Taiwan, R.O.C.
[2]Iron and Steel R&D Department, China Steel Corporation,
Kaohsiung, Taiwan, R.O.C.

Keywords: Niobium, Coarse Grained Heat Affected Zone, Thermal Simulation, Widmanstätten Ferrite, Bainite, Interlocking Ferrite Structure, TEM, Heat Input, Charpy Toughness, Microstructure, Phase Transformation

Abstract

With the purpose of evaluating the effect of niobium additions on the microstructures of the HAZ (heat-affected zone) in mild steels, a plain C-Mn steel (without niobium) and three niobium containing steels with 0.01, 0.02 and 0.04 wt%Nb respectively, were investigated through simulated HAZ experiments at heat inputs of 20, 50 and 80 kJ/cm. The microstructures of simulated coarse-grained HAZ's have been examined by optical metallography and transmission electron microscopy. It was found that the addition of niobium had a significant effect on the transformation in the HAZ. For high energy heat inputs (80 and 50 kJ/cm), the addition of niobium retarded the pearlite formation, even in the case of the 0.01 wt%Nb containing steel. The microstructures of the coarse-grained HAZ of niobium-containing steels consisted mainly of secondary Widmanstätten ferrite, but that of the niobium-free steel contained a large amount of pearlite as well as secondary Widmanstätten ferrite. At the low energy heat input level (20 kJ/cm), the microstructures of the coarse-grained HAZ of the niobium-containing steels were all similar and consisted mainly of interlocking ferrite plates with small amounts of bainite and Widmanstätten ferrite; while that of the niobium-free steel comprised Widmanstätten ferrite and martensite with a small quantity of pearlite. The results from Charpy impact tests indicated that the niobium-containing steels with a simulated HAZ heat input of 20 kJ/cm possessed higher toughness than those treated at heat inputs of 50 and 80 kJ/cm. It is proposed that the interlocking ferrite structure, which forms in the HAZ of the niobium-containing steels after simulation of a 20 kJ/cm heat input level, improves the toughness property.

Introduction

Nb-microalloyed steels have been studied extensively over the past four decades. Plenty of investigators have studied austenite recrystallisation behaviour in these kinds of steels, and have shown that the addition of Nb can substantially retard the recrystalisation of austenite during hot rolling [1-3]. It is well known that the principal strengthening of these steels is derived from precipitation of finely dispersed niobium carbonitrides Nb(CN) in a ferrite matrix. Nb(CN) can also be utilised in the refinement of austenite grains if austenite conditioning has been controlled. The use of these products, which have been applied in such areas as ships, buildings, automotive and earthmoving equipment and pipelines etc., usually involves fabrication by welding. It is known that high-energy welding processes such as submerged-arc or electro-slag welding usually cause a brittle microstructure in the heat-affected zone (HAZ) of niobium-containing steels [4,5]. At the highest range of temperatures in the weld thermal cycle, niobium carbonitrides, which are effective in pinning the austenite grain-boundaries, tend to dissolve. This results in rapid coarsening of austenite grains in the HAZ adjacent to the fusion line. Niobium taken into solid-solution in coarse-grained austenite will have a strong effect on the subsequent transformation [6-9]. Some researchers have studied the HAZ of niobium-containing steels [10-13], however, considerable confusion exists in the literature, particularly with regard to the effect of niobium on the microstructural morphology in the HAZ. The classification of microstructures, on the basis of morphology, is of considerable use in the study of structure-property relationships. Therefore further studies are needed to clearly characterise the various ferrite morphologies in the HAZ.

The aim of the present work is to determine the effect of niobium additions on the coarse-grained HAZ microstructures after thermal simulations performed on a Gleeble 1500 machine (manufactured by Duffers Scientific, Inc.). The toughness of each microstructure has also been evaluated in order to define the relationship between microstructure and toughness.

Experimental Procedure

The investigation involved four different steels. A plain C-Mn steel was selected as the reference material. To find out the effect of Nb addition, three other steels with the same C-Mn base composition but alloyed with 0.01, 0.02 and 0.039 wt%Nb respectively, were also investigated. The chemical compositions of the steels are given in Table I; the reference steel (without Nb) is designated as steel O, and the 0.01, 0.02 and 0.039 wt%Nb containing steels identified as L, M and H, respectively. All steels were prepared by vacuum melting, then cast into 100 kg ingots with a thickness of 210 mm. The ingots were homogenised at 1200 °C for 2 h and then hot rolled in several passes, by 20% reduction per pass, to plates of 20 mm thickness with a finishing temperature of 850 °C. The plates were air cooled to room temperature after hot rolling.

Table I. Chemical Compositions (wt%) of the Steels Studied

Steel	C	Si	Mn	P	S	Nb	Al	N*
O	0.127	0.29	1.36	0.017	0.008	-	0.029	54
L	0.128	0.29	1.47	0.018	0.008	0.010	0.032	83
M	0.124	0.30	1.37	0.017	0.008	0.020	0.037	54
H	0.125	0.29	1.36	0.017	0.008	0.039	0.031	56

*N in ppm

The simulated HAZ experiments were carried out on a Gleeble 1500 machine. Before thermal simulation, the representative weld thermal cycles from actual welding had been obtained as described below. Test beads were deposited on 20 mm thick steel plates, using the bead on plate technique, by submerged-arc welding at three different heat inputs: 20, 50 and 80 kJ/cm. The thermal cycles were measured at the location of the coarse-grained region in the HAZ close to the fusion boundary. The thermal cycles are shown in Figure 1; the peak temperatures were approaching 1400 °C for the three cycles and cooling times between 800 and 500 °C ($\Delta t_{8/5}$) for the heat inputs of 80, 50 and 20 kJ/cm were 220, 102 and 16 s, respectively. The specimens to be used for simulation were sectioned from the as-rolled plates along the rolling direction as bars of dimensions 11 x 11 x 56 mm. A Gleeble 1500 machine was employed to reproduce repesentative coarse grained HAZ microstructures in the samples. After the Gleeble thermal simulation cycles, the Charpy specimens were prepared in the standard form of 10 x 10 x 55 mm. Notches were located in the uniform microstructural region at the centre of the specimens and Charpy impact tests were carried out at 0, -20, -40 and -60 °C.

The optical metallography specimens were prepared from the coarse-grained HAZ region of Charpy specimens. The specimens were mechanically polished and then etched in 2% Nital solution. Hardness measurements were made on optical specimens using a Vickers hardness tester. A load of 300 g was used in order to make the indentation on the individual phases. Transmission electron microscopy samples were prepared from 0.25 mm thick discs slit from the coarse grained HAZ region of the Charpy specimens. The discs were mechanically ground down to a thickness of 0.05 mm on 1200 grit SiC paper; the specimens were then single-jet electropolished using a 5% perchloric acid, 25% glycerol and 70% ethanol mixture at ambient temperature and 60 V polishing potential. The electron microscopy was carried out using a JEM 2000 EX transmission electron microscope operated at 200 kV.

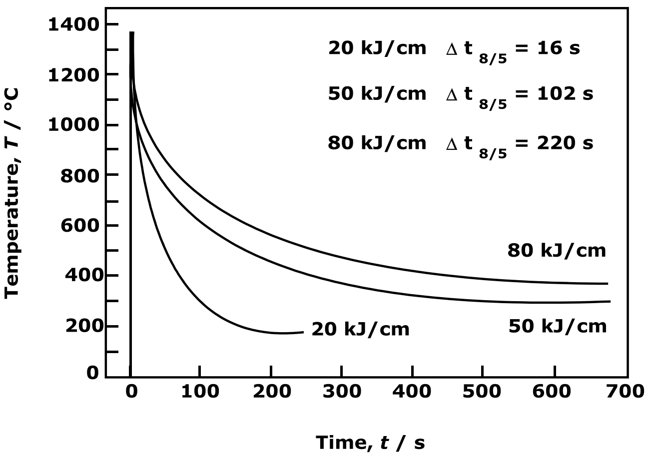

Figure 1. Thermal cycles of HAZ simulations corresponding to the real thermal cycles for three heat inputs: 80, 50 and 20 kJ/cm.

Results and Discussion

Optical Metallography

The optical microstructures of the as-rolled steels were all similar, and consisted of banded structures of equiaxed ferrite and pearlite as shown in Figures 2(a) and (b). Steel H possessed the smallest ferrite grain size (about 20 μm) of the three niobium containing steels studied. The electron micrographs, Figures 2(c) and (d), revealed large quantities of fine niobium carbonitride particles scattered in the ferrite matrix. The high ingot reheating temperature (1200 °C) allowed most of the niobium carbonitrides to dissolve in the austenite as the maximum solubility of niobium in steel H is about 0.037 wt% in austenite, based on the solubility product equation for NbC proposed by Irvine et al. [8] as follows:

$$\log[Nb][C] = -6770/T+2.26, \qquad (1)$$

where the solubilities are expressed in wt% as a function of absolute temperature.

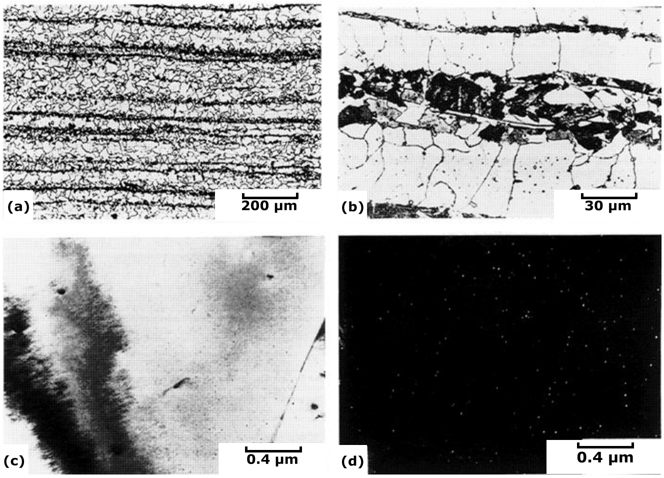

Figure 2. Microstructure of the as-rolled steel H; (a) and (b): Optical micrographs, (c) and (d): Bright and dark field images from electron micrographs.

In microalloyed steels, where strong carbide-forming elements are present in concentrations less than 0.1 wt%, it is often possible to obtain the ferrite in a supersaturated condition with little or no carbide precipitation taking place during the $\gamma \rightarrow \alpha$ reaction [14]. However, in the thermo-mechanical process for producing the as-rolled steel H, the finish-rolling at a low temperature (850 °C) would accumulate strain in the deformed austenite and promote the very finely dispersed niobium carbonitride precipitates as observed in this steel (0.039 wt%Nb). Indeed, while the steel was cooled through the transformation temperature of ferrite, carbide particles formed in the ferrite matrix due to interface precipitation.

The typical structure in a low-alloy steel HAZ is characterised by a very coarse prior austenite grain size with allotriomorphic ferrite layers formed during cooling after welding. The allotriomorphic ferrite which nucleates at the prior austenite grain boundaries tends to grow along the austenite boundaries at a rate faster than in the direction normal to the boundary plane. When the cooling time from 800 to 500 °C is short, the layers of allotriomorphic ferrite become thin or even disappear. It is believed [15,16] that during continuous cooling, the transformation temperature of Widmanstätten ferrite is just below that of allotriomorphic ferrite. In the coarse-grained region of the HAZ, there are usually two kinds of Widmanstätten ferrite to be found, primary and secondary Widmanstätten ferrite [15,17]. Secondary Widmanstätten ferrite nucleates at the allotriomorphic ferrite/austenite boundaries and grows as sets of parallel plates separated by thin layers of austenite, the latter subsequently being retained to ambient temperature or partially transforming to martensite and/or pearlite. On the other hand, primary Widmanstätten ferrite nucleates directly from austenite grain boundaries which are not covered by allotriomorphic ferrite, although its growth mechanism is identical to that of secondary Widmanstätten ferrite. Details of the transformation mechanism of Widmanstätten ferrite have been reported in Reference [18]. In Dubé`s classification [19], secondary Widmanstätten ferrite was referred to as a ‘Widmanstätten ferrite side-plate’ and primary Widmanstätten ferrite was called a ‘Widmanstätten ferrite primary side-plate’.

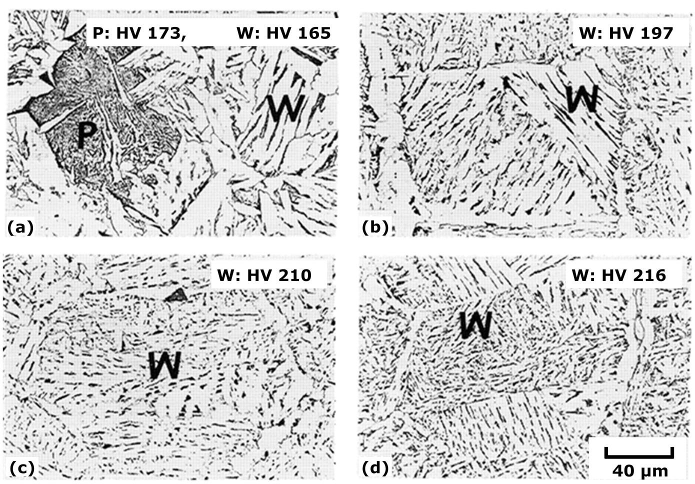

Figure 3. Optical micrographs obtained from four different steels after a simulated HAZ thermal cycle at 80 kJ/cm; (a) steel O, (b) steel L, (c) steel M and (d) steel H. Value of Vickers hardness, HV, for each phase is indicated. (W: Widmanstätten ferrite; P: pearlite).

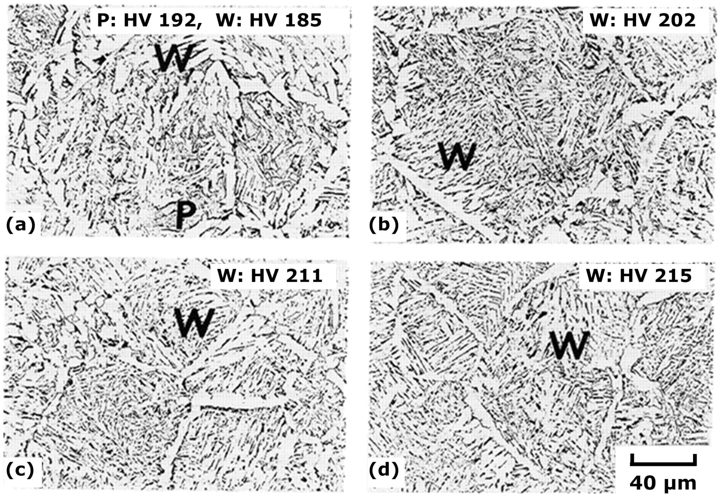

Figure 4. Optical micrographs obtained from four different steels after a simulated HAZ thermal cycle at 50 kJ/cm; (a) steel O, (b) steel L, (c) steel M and (d) steel H. Value of Vickers hardness, HV, for each phase is indicated. (W: Widmanstätten ferrite; P: pearlite).

The structures of the coarse-grained HAZ in the niobium-containing steels and the reference steel without Nb are significantly different, especially in the case of high energy inputs, 80 and 50 kJ/cm, and their corresponding optical micrographs are presented in Figures 3 and 4. Figure 3 shows that after 80 kJ/cm heat input, the HAZ microstructure of steel O, without Nb, Figure 3(a), was composed of large amounts of pearlite colonies with secondary Widmanstätten ferrite (containing a coarse layer of allotriomorphic ferrite). Whereas, after 80 kJ/cm heat input, the microstructures of steel L, 0.01 wt%Nb, Figure 3(b), steel M, 0.02 wt%Nb, Figure 3(c), and steel H, 0.039 wt%Nb, Figure 3(d), consisted mainly of secondary Widmanstätten ferrite (containing a thin layer of allotriomorphic ferrite) and retained microphases trapped between the Widmanstätten ferrite plates. The results from optical metallography imply that the small additions of niobium brought about the retardation of the $\gamma \rightarrow \alpha$ transformation kinetics. Consequently, pearlite colonies do not exist in the niobium-containing steels even after 80 kJ/cm heat input, which has a long cooling time between 800 to 500 °C of 220 s. The above results are consistent with those reported by several authors [20,21]. They claimed that small additions of niobium in solid solution in austenite would increase the hardenability of the steel. It has been suggested that because the niobium atoms have a large misfit within the iron lattice, the austenite grain boundaries are favourable sites for the location of niobium atoms. Grain-boundary segregation of niobium is presumed to raise the energy barrier to ferrite nucleation at the austenite grain boundaries; therefore, niobium has a strong retarding effect on the transformation of austenite to allotriomorphic ferrite and pearlite [21].

By comparing the micrographs in Figure 3 and Figure 4, it can be seen that, for the steels studied, the effect of Nb on $\gamma \rightarrow \alpha$ transformation after 50 kJ/cm heat input simulation is similar to that at 80 kJ/cm heat input. The above results indicate that under the conditions of 80 kJ/cm and 50 kJ/cm, additions of niobium retard the pearlite transformation. On the other hand, at a low energy heat input, 20 kJ/cm, the microstructure of the coarse-grained HAZ of niobium-containing steels consisted chiefly of interlocking ferrite plates with small amounts of bainite and Widmanstätten ferrite, Figures 5(b)–(d); while that of the niobium-free steel comprised Widmanstätten ferrite and martensite with a small fraction of pearlite, Figure 5(a).

At heat inputs of 80 kJ/cm and 50 kJ/cm, the secondary Widmanstätten ferrite can be obtained in all the steels studied as shown in Figures 3 and 4; whereas, at the heat input of 20 kJ/cm, the primary Widmanstätten ferrite replaces the secondary Widmanstätten ferrite as shown in Figure 5. The results indicate that at a slow cooling rate between 800 and 500 °C the formation of allotriomorphic ferrite may occur before that of Widmanstätten ferrite (i.e., secondary Widmanstätten ferrite forms). The evidence from optical metallography, Figures 3 and 4, also indicates that small additions of niobium have a significant effect on the secondary Widmanstätten ferrite transformation. For the same heat input, the width of the Widmanstätten ferrite plates in the niobium-free steel is much coarser as compared with that in the niobium-containing steels. Micralloyed niobium does depress the transformation start temperature of Widmanstätten ferrite, as a result, the width of the Widmanstätten ferrite plates in the niobium-containing steels becomes finer.

The major effect of niobium on HAZ microstructure in the case of the 20 kJ/cm heat input level appears to be the formation of interlocking ferrite plates, Figures 5(b)–(d). A similar structure is well known to be acicular ferrite in alloy-steel weld deposits [22], where non-metallic inclusions play an important role in development of intragranular nucleation. Another similar structure of intersecting acicular ferrite [23,24], which forms in deformed austenite under controlled-rolling and accelerated-cooling, has also been reported. The detailed morphology and toughness properties of the interlocking ferrite plates will be discussed in the following sections.

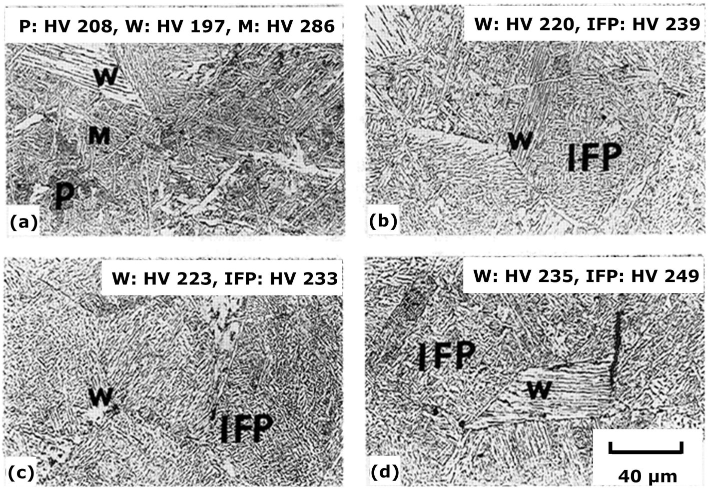

Figure 5. Optical micrographs obtained from four different steels after a simulated HAZ thermal cycle at 20 kJ/cm; (a) steel O, (b) steel L, (c) steel M and (d) steel H. Value of Vickers hardness, HV, for each phase is indicated. (W: Widmanstätten ferrite; M: martensite; P: pearlite; IPF: interlocking ferrite plates).

<u>Transmission Electron Microscopy</u>

In the optical micrographs, it is very difficult to reveal the microstructural details of the bainite, martensite and the interlocking ferrite plates. Attention was therefore focused on transmission electron microscopy. The electron micrograph shown in Figure 6 was taken from the 20 kJ/cm heat input specimen of steel H. It clearly illustrates the characteristics of the interlocking ferrite plates, which are usually found in the niobium containing steel specimens after simulation of 20 kJ/cm heat input, such as the regions marked **IFP** in Figures 5(b), (c) and (d). Figure 6 reveals that the individual interlocking ferrite plate has a high dislocation density which implies that the transformation mechanism could be displacive. In the upper left-hand region of the micrograph, a lower bainite plate (with intra-plate carbides precipitated in a single variant) can be found. Figure 7 illustrates transmission electron micrographs and corresponding diffraction patterns for the interlocking structures. The dark-field images, as shown in Figures 7(b) and (c), illuminate the packet structures which are made up of several parallel plates having essentially the same orientation. The orientation relationship between these two packets of interlocking ferrite plates has been investigated by analysing the corresponding electron diffraction patterns, as shown in Figure 7(e). The result is illustrated in Table II, where 24 equivalent axis-angle pairs relating these two packets of ferrite plates are shown. Judging from the highest angle of rotation, [0.0000 0.1524 0.9883]/180°, it appears that the orientation relationship between these two packets of interlocking ferrite plates may result from the existence of a Nishiyama-Wasserman orientation relationship with austenite, which has been documented in Reference [25]. The result indicates that the transformation mechanism of the interlocking ferrite has a displacive characteristic. Widmanstätten ferrite also forms by a displacive mechanism, but it grows as sets of parallel plates without interlocking or intersecting. The morphology of interlocking ferrite plates is distinct from that of Widmanstätten ferrite; the former essentially forms through intragranular nucleation so that its distinctive feature can be developed. It has been claimed [26,27] that in HAZ structures of titanium-containing steels, titanium oxides and nitrides act as favourable nucleation sites for intra-granular ferrite plates within prior austenite grains. In this work, the nucleation mechanism of the interlocking ferrite plates involved is not yet understood.

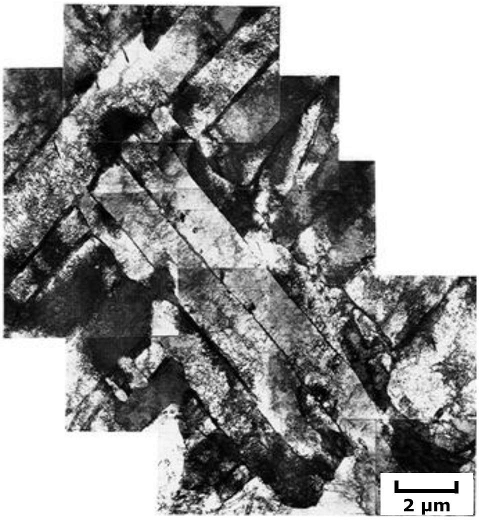

Figure 6. Transmission electron micrograph showing the interlocking structures obtained from steel H specimen after a simulated HAZ thermal cycle at 20 kJ/cm.

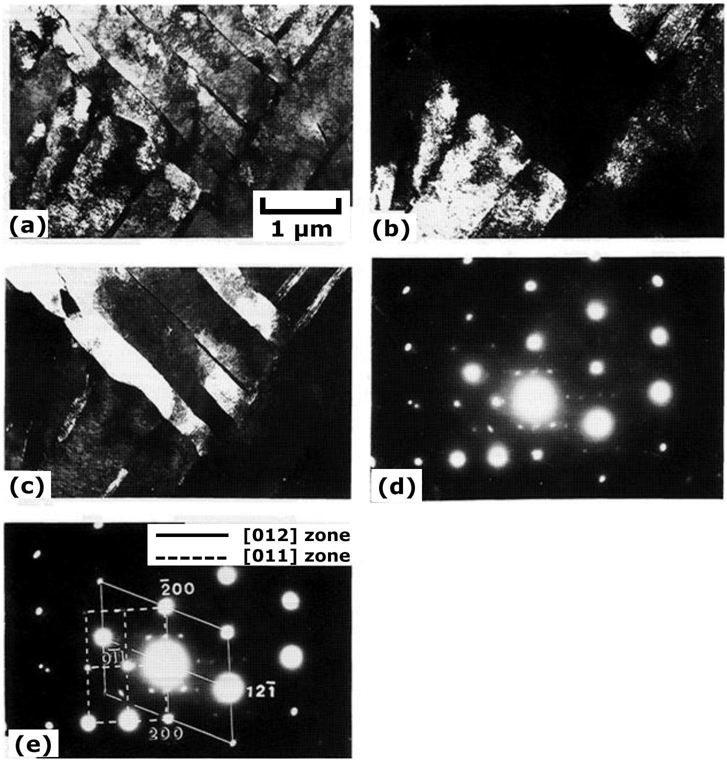

Figure 7. Transmission electron micrographs and corresponding diffraction patterns illustrating the interlocking structures; (a) bright field image, (b) and (c) dark field images, (d) corresponding diffraction pattern, (e) interpretation of (d).

Table II. 24 Equivalent Axis-Angle Pairs Relating Two Packets of Interlocking Ferrite Structure

No.	Axis			Angle (°)
1	1.0000	0.0000	0.0000	17.5
2	-0.5089	-0.6943	-0.5089	110.5
3	0.6278	0.6278	0.4601	130.6
4	0.0000	0.5911	0.8066	180.0
5	-0.7029	0.7029	-0.1084	167.6
6	-0.7029	0.1084	0.7029	167.6
7	-1.0000	0.0000	0.0000	72.5
8	0.1506	0.9771	-0.1506	91.3
9	-0.7029	-0.7029	0.1084	167.6
10	0.6278	-0.6278	0.4601	130.6
11	0.6278	-0.4601	0.6278	130.6
12	0.0000	0.1524	0.9883	180.0
13	1.0000	0.0000	0.0000	107.5
14	-0.7029	-0.1084	-0.7029	167.6
15	0.1506	-0.1506	0.9771	91.3
16	-0.5089	0.6943	0.5089	110.5
17	-0.5089	-0.5089	0.6943	110.5
18	0.0000	0.9883	0.1524	180.0
19	0.1506	-0.9771	0.1506	91.3
20	0.0000	0.8066	0.5911	180.0
21	0.1506	0.1506	0.9771	91.3
22	0.6278	0.4601	-0.6278	130.6
23	-0.5089	0.5089	-0.6943	110.5
24	-1.0000	0.0000	0.0000	162.5

Some of the microstructural features from the simulated HAZ specimens have also been studied by transmission electron microscopy. They are illustrated in Figures 8 to 12. Figure 8 shows the microstructure obtained from steel O after 80 kJ/cm heat input simulation. The corresponding optical micrograph is shown in Figure 3(a). It shows that pearlite and Widmanstätten ferrite transformed from the austenite after allotriomorphic ferrite grew from the prior austenite grain boundaries during the thermal cycle. Pearlitic structures were not found in the niobium containing steels studied under the same heat input. It is clear that with Nb in solid solution in austenite, a pearlite structure cannot be obtained even at the slow cooling rate associated with a 80 kJ/cm heat input. The result is consistent with the reports by several authors [8,10,12] who asserted that addition of a suitable amount of niobium (less than 0.04 wt%) increases the hardenability of steels. Figure 9 shows the microstructure obtained from steel H after a 50 kJ/cm heat input simulation. Its corresponding optical micrograph is shown in Figure 4(d). Secondary Widmanstätten ferrite nucleated at the allotriomorphic ferrite-austenite boundaries and grew as sets of parallel plates separated by thin regions of austenite, the latter subsequently being retained to ambient temperature or partially transforming to martensite, Figure 9(b). These small quantities of retained austenite and martensite mixtures are called M/A constituents. Abson et al. [28] therefore refer to this Widmanstätten ferrite and its associated microphases as "Ferrite with Aligned Martensite Austenite-Carbide". As to the mechanical properties, Widmanstätten ferrite in the HAZ is generally regarded as an undesirable constituent because its presence leads to poor toughness; the longer the plates of Widmanstätten ferrite, the poorer the toughness. Figures 10 to 12 (obtained from steel H after a heat input simuation of 20 kJ/cm) show separately, upper bainite, lower bainite and autotempered martensite. It is well known that upper bainite is more brittle than lower bainite. Cleavage fracture is definitely controlled by both the carbide particle size and morphology. The interplate carbides are much coarser in upper bainite and crack easily under the influence of the stress which accumulates as carbides block an active slip band. In steel H the martensite start temperature is about 445 °C and martensite formed at higher temperatures will be autotempered [29]. Autotempered martensite plates are also expected to possess good toughness due to the more uniform distribution of fine carbide particles within their plates. In the 20 kJ/cm heat input simulation specimens of niobium-containing steels, the amounts of bainite and autotempered martensite are very small. Optical micrographs in Figures 5(b) to (d) have shown that for a 20 kJ/cm heat input, the microstructures of the coarse-grained HAZ of niobium-containing steels consisted chiefly of interlocking ferrite plates with small amounts of bainite and Widmanstätten ferrite. Indeed, it is very difficult to distinguish lower bainite from autotempered martensite in the optical micrograph since both phases tend to produce grey etching structures owing to the existence of interplate or interlath carbides.

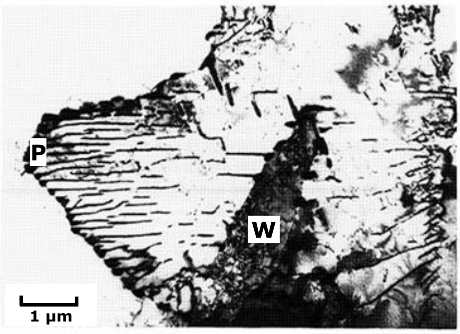

Figure 8. Transmission electron micrograph showing Widmanstätten ferrite obtained from steel O sample after a simulated HAZ thermal cycle at 80 kJ/cm (W: Widmanstätten ferrite; P: pearlite).

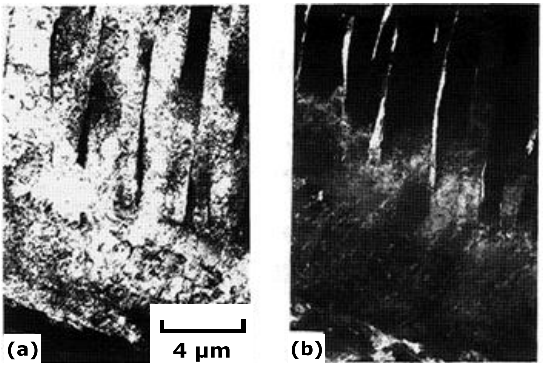

Figure 9. Transmission electron micrographs; (a) bright field and (b) dark field images showing secondary Widmanstätten ferrite obtained from steel H sample after a simulated HAZ thermal cycle at 80 kJ/cm.

Figure 10. Transmission electron micrograph showing upper bainite obtained from steel H sample after a simulated HAZ thermal cycle at 20 kJ/cm.

Figure 11. Transmission electron micrograph showing lower bainite obtained from steel H sample after a simulated HAZ thermal cycle at 20 kJ/cm.

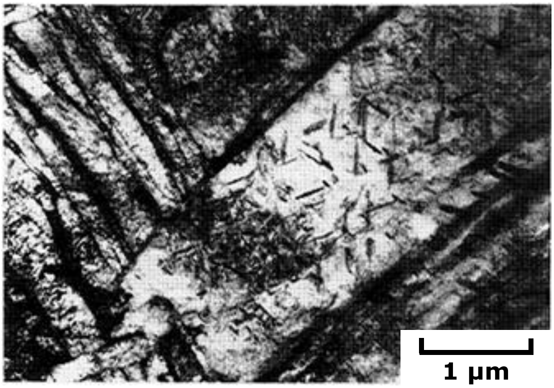

Figure 12. Transmission electron micrograph showing autotempered martensite obtained from steel H sample after a simulated HAZ thermal cycle at 20 kJ/cm.

It is well known that after a high-energy welding process such as submerged-arc or electro-slag welding, the HAZ of niobium-containing steels gives a typical structure of secondary Widmanstätten ferrite. Several authors have asserted [10,20,30] that the effect of niobium on transformation behaviour has been noted as the emergence of the acicular ferrite or bainite. However, there is no detailed transmission electron microscopy to identify the morphologies of acicular ferrite and bainite. The classification of microstructures on the basis of morphology is of considerable importance in the study of structure-property relationships. More research work on this aspect is needed.

Charpy Impact Test

Figure 13 presents the variation of Charpy impact energy as a function of test temperature for the simulated HAZ specimens. At 80 kJ/cm and 50 kJ/cm heat inputs, the niobium containing steels (steels H, M and L) and the niobium-free steel (steel O), possess nearly the same toughness at subzero temperatures as shown in Figures l3(a) and (b). However, at the 20 kJ/cm heat input level, the niobium containing steels have much higher toughness than the niobium-free steel as shown in Figure 13(c). The data also indicates that for the same niobium containing steel the specimens obtained from the simulation of a heat input of 20 kJ/cm possess higher toughness than those obtained from the simulations of heat inputs of 50 kJ/cm and 80 kJ/cm. This result is consistent with the published work [27], which demonstrates that at lower heat inputs an improved toughness is obtained if niobium is added to the steel.

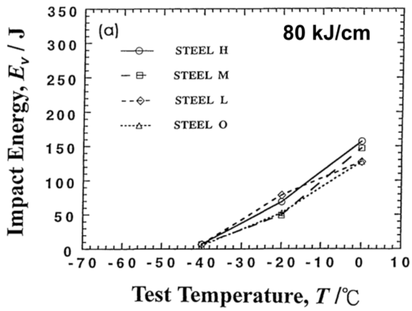

(a)

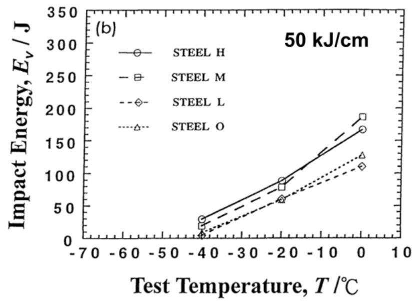

(b)

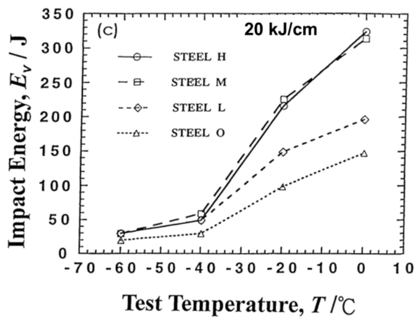

(c)

Figure 13. Plots of Charpy impact energy versus test temperature for four different steels after simulated HAZ thermal cycles at (a) 80 kJ/cm, (b) 50 kJ/cm and (c) 20 kJ/cm.

In the present work the results reflect that the interlocking ferrite structure, which forms in the niobium containing steels after 20 kJ/cm heat input simulation, improves the toughness property. Most studies of low-carbon steels agree that the important structural unit affecting toughness is the cleavage facet size since the cleavage crack is deflected at the packet boundaries. Each packet consists of a group of platelets, which have habit plane poles in close proximity and are essentially the same crystallographic orientation. It is conceivable that the transformation crystallography is vital because this exerts an influence on both the packet size and morphology. Widmanstätten ferrite, having a set of extremely long and parallel ferrite plates in identical orientation, is detrimental to toughness. Indeed, Widmanstätten ferrite leads to a more general condition that groups of plates with a common cleavage plane should be avoided. On the other hand, the reason why the structure of interlocking ferrite plates is a desirable microstructural constituent can be understood as follows. This structure possesses much finer packets which consist of several small platelets; adjacent packets have different habit planes and are different variants of the Nishiyama-Wasserman orientation relationship with austenite. It is suggested that the refinement of packets causes substantial crack deflections and hence improves the toughness of the interlocking ferrite plates microstructure.

Conclusions

An investigation has been made of the simulated heat-affected zone (HAZ) using thermal cycles equivalent to heat inputs of 20 kJ/cm, 50 kJ/cm and 80 kJ/cm in niobium-free and niobium-containing steels. The thermal cycles used corresponded to the actual thermal cycles that occur in the coarse grained region of the real HAZ. The microstructure and toughness of the simulated HAZ have been studied. The important conclusions of this work may be summarised as follows:

1. The results indicate that the addition of niobium can retard the pearlite formation in the steels studied for heat inputs of 50 kJ/cm and 80 kJ/cm; the corresponding microstructures in the coarse-grained region in the niobium containing steels consisted mainly of typical Widmanstätten ferrite, but that in the niobium-free steel was composed of a large amount of pearlite with some Widmanstätten ferrite.

2. At the low energy heat input level (20 kJ/cm), the microstructures in the HAZ of the niobium containing steels consisted mainly of interlocking ferrite plates with a small amount of bainite and Widmanstätten ferrite; whereas the niobium-free steel also contained a small quantity of pearlite.

3. At 80 kJ/cm and 50 kJ/cm heat inputs, the niobium containing steels and the niobium-free steel possessed approximately the same toughness at subzero temperatures. However, at the 20 kJ/cm heat input, the niobium containing steels had much higher toughness than the niobium-free steel. The evidence reflects that the interlocking ferrite structure, which forms in niobium-containing steels after the 20 kJ/cm heat input simulation, improves the Charpy impact toughness property.

Acknowledgement

This work was carried out with the financial support from China Steel Corporation. The authors thank China Steel Corporation for the supply of the steel plates.

References

1. M.J. Crooks et al., “Precipitation and Recrystallization in Some Vanadium and Vanadium-niobium Microalloyed Steels,” *Metallurgical Transactions A*, 12 (12) (1981), 1999-2013.

2. H. Abrams et al., *HSLA Steels: Metallurgy and Applications*, (Philadelphia, PA: ASM, 1986), 579.

3. S.S. Hansen, J.B. Vander Sande, and M. Cohen, “Niobium Carbonitride Precipitation and Austenite Recrystallization in Hot-rolled Microalloyed Steels,” *Metallurgical Transactions A,* 11 (3) (1982), 387-402.

4. H. Nakasugi, H. Matsuda, and H. Tamehiro, *Steels for Line Pipe and Pipe Line Fittings* (London, UK: Metals Society, 1981), 90-95.

5. H. Ohtani, T. Hashimoto, and T. Kyogoku, *HSLA Technology and Applications* (Philadelphia, PA: ASM, 1983), 843.

6. D. Webster and J.H. Woodhead, “Effect of 0.03% Niobium on the Ferrite Grain Size of Mild Steel,” *Journal of the Iron and Steel Institute*, 202 (1964), 987-994.

7. G.T. Eldis and W.C. Hage, *Hardenability Concepts with Application to Steels*, (Warrendale, PA: TMS-AIME, 1978), 397-420.

8. K.J. Irvine, F.B. Pickering, and T. Gladman, “Grain-refined C-Mn Steels,” *Journal of the Iron and Steel Instiute*, 205 (2) (1967), 161-165.

9. C. Fossaert et al., “The Effect of Niobium on the Hardenability of Microalloyed Austenite,” *Metallurgical and Materials Transactions A,* 26 (1) (1995), 21-30.

10. N. Shams, “Microstructure of Continuous Cooled Niobium Steels,” 37 (12) (1985), 21-24.

11. R. Otterberg, R. Sandstrom, and R. Sandberg, “Influence of Widmanstätten Ferrite on Mechanical Properties of Microalloyed Steels,” *Metals Technology*, 7 (1) (1980), 397-408.

12. S. Suzuki, G.C. Weatherly, and D.C. Houghton, “The Response of Carbo-nitride Particles in HSLA Steels to Weld Thermal Cycles,” *Acta Metallurgica*, 35 (2) (1987), 341-352.

13. J. Strid and K.E. Easterling, “On the Chemistry and Stability of Complex Carbides and Nitrides in Microalloyed Steels,” *Acta Metallurgica*, 33 (11) (1985), 2057-2074.

14. R.W.K. Honeycombe and H.K.D.H. Bhadeshia, *Steels - Microstructure and Properties*, 2nd edition, (London, UK: Edward Arnold, 1995), 76.

15. H.K.D.H. Bhadeshia, L-E. Svensson, and B. Gretoft, “A Model for the Development of Microstructure in Low-alloy Steel (Fe-Mn-Si-C) Weld Deposits,” *Acta Metallurgica*, 33 (7) (1985), 1271-1283.

16. L. Levine and D.C. Hill, “Structure-property Relationships in Low C Weld Metal,” *Metallurgical Transactions A*, 8 (9) (1977), 1453-1463.

17. J.R. Yang and L.C. Chang, “The Effect of Stress on the Widmanstätten Ferrite Transformation,” *Materials Science and Engineering A*, 223 (1) (1997), 158-167.

18. H.K.D.H. Bhadeshia, “A Rationalisation of Shear Transformations in Steels,” *Acta Metallurgica*, 29 (6) (1981), 1117-1130.

19. C.A. Dube, H.I. Aaronson, and R.F. Mehl, “La Formation de la Ferrite Proeutectoide dans les Aciers au Carbone,” *Revue de Metallurgie*, 55 (1958), 201-210.

20. A.J. DeArdo, J.M. Gray, and L. Meyer, *Fundamental Metallurgy of Niobium in Steel* Niobium, (Warrendale, PA: TMS—AIME, 1984), 685-759.

21. C. Fossaert et al., “The Effect of Niobium on the Hardenability of Microalloyed Austenite,” *Metallurgical and Materials Transactions A*, 26 (1) (1995), 21-30.

22. J.R. Yang and H.K.D.H. Bhadeshia, “Continuous Heating Transformation of Bainite to Austenite,” *Materials Science and Engineering A*, 131 (1) (1991), 99-113.

23. J.R. Yang, C.Y. Huang, and C.S. Chiou, “The Influence of Plastic Deformation and Cooling Rates on the Microstructural Constituents of an Ultra-low Carbon Bainitic Steel,” *Iron and Steel Institute of Japan International*, 35 (8) (1995), 1013-1019.

24. Z. Huang and M. Yao, “Effect of Arrangement of Acicular Ferrite in a Widmanstatten Microstructure on the Fracture of Mild Steel,” *Materials Science and Engineering* A, 119 (1989), 211-217.

25. J.R. Yang and H.K.D.H. Bhadeshia, “Orientation Relationships between Adjacent Plates of Acicular Ferrite in Steel Weld Deposits,” *Materials Science and Technology*, 5 (1) (1989), 93-97.

26. F.J. Barbaro, P. Krauklis, and K.E. Easterling, “Formation of Acicular Ferrite at Oxide Particles in Steels,” *Materials Science and Technology*, 5 (11) (1989), 1057-1068.

27. Ø. Grong and O.M. Akselsen, “HAZ Toughness of Micralloyed Steels for Offshore,” *Metal Construction*, 18 (9) (1986), 557-562.

28. D.J. Abson and R.E. Dolby, (Document, IXJ-29-80, International Institute of Welding, 1980), 1.

29. R.W.K. Honeycombe and H.K.D.H. Bhadeshia, *Steels-Microstructure and Properties*, 2nd edition, (London, UK: Edward Arnold, 1995), 171.

30. J.M. Gray, “Weldability of Niobium Containing High Strength Low Alloy Steel,” *Welding Research Council Bulletin*, 213 (1976), 1.